JACS
JOURNAL OF THE AMERICAN CHEMICAL SOCIETY

Communication

pubs.acs.org/JACS

Protein Delivery of a Ni Catalyst to Photosystem I for Light-Driven Hydrogen Production

Sunshine C. Silver, Jens Niklas, Pingwu Du,† Oleg G. Poluektov, David M. Tiede,* and Lisa M. Utschig*

Chemical Sciences and Engineering Division, Argonne National Laboratory, Argonne, Illinois 60439, United States

Supporting Information

ABSTRACT: The direct conversion of sunlight into fuel is a promising means for the production of storable renewable energy. Herein, we use Nature's specialized photosynthetic machinery found in the Photosystem I (PSI) protein to drive solar fuel production from a nickel diphosphine molecular catalyst. Upon exposure to visible light, a self-assembled PSI-$[Ni(P_2^{Ph}N_2^{Ph})_2](BF_4)_2$ hybrid generates H_2 at a rate 2 orders of magnitude greater than rates reported for photosensitizer/$[Ni(P_2^{Ph}N_2^{Ph})_2](BF_4)_2$ systems. The protein environment enables photocatalysis at pH 6.3 in completely aqueous conditions. In addition, we have developed a strategy for incorporating the Ni molecular catalyst with the native acceptor protein of PSI, flavodoxin. Photocatalysis experiments with this modified flavodoxin demonstrate a new mechanism for biohybrid creation that involves protein-directed delivery of a molecular catalyst to the reducing side of Photosystem I for light-driven catalysis. This work further establishes strategies for constructing functional, inexpensive, earth-abundant solar fuel-producing PSI hybrids that use light to rapidly produce hydrogen directly from water.

Sunlight is an abundant and environmentally clean resource that, when harnessed as an energy source, can help meet increasing global energy demands and decrease our reliance on fossil fuels. Current solar fuel research involves the creation of new materials that can effectively capture sunlight and convert it into a storable fuel so that the energy from the sun can be used when needed.[1−3] The most efficient way to store solar-converted energy is in the form of energy-rich chemical bonds of molecules such as hydrogen or oxygen, and the ideal strategy to accomplish this uses water, visible light, and earth-abundant materials. Nature provides a model of this. In photosynthesis, the energy from sunlight is used to rearrange bonds of water to form oxygen and an equivalent of hydrogen, NADPH.[4] Nature accomplishes solar energy conversion by using finely tuned protein−pigment complexes called photosynthetic reaction centers (RCs). New experimental strategies for solar hydrogen generation couple light-driven RC chemistry to the direct synthesis of hydrogen in hybrid systems wherein hydrogen catalysts have been inserted into the RC protein framework.[5−8] Here we describe the first example of a hybrid incorporating a synthetic molecular nickel catalyst wherein hydrogen formation is driven by light-induced electron transfer of the Photosystem I (PSI) RC protein.

Recently, we reported a first-of-its-kind solar fuel hybrid architecture that uses a synthetic *molecular cobalt* catalyst linked to PSI photochemistry.[8] This novel structure was realized by simple self-assembly of PSI with a well-known molecular hydrogen cobaloxime electrocatalyst, $Co(dmgH)_2pyCl$ (where dmgH = dimethylgloximate, py = pyridine).[9] Now we extend this work to show its applicability to a *molecular nickel* catalyst. In general, designs using first-row transition metal catalysts, such as cobalt and nickel complexes, provide a low-cost alternative to traditional hydrogen catalysts comprised of rare and expensive metals, such as colloidal platinum. DuBois and co-workers have synthesized a series of highly active nickel electrocatalysts that rapidly produce hydrogen at low pH in nonaqueous solutions.[10−12] The first example of photogeneration of hydrogen from one of these nickel diphosphine catalysts, $[Ni(P_2^{Ph}N_2^{Ph})_2](BF_4)_2$, has been demonstrated at pH 2 using synthetic photosensitizer molecules as light-harvesters and photoreductants and ascorbic acid as an electron donor.[13] An interesting experimental question is whether a protein environment will allow photocatalysis to be achieved in completely aqueous conditions at near-neutral pH for a nickel diphosphine catalyst. Herein, we report methods for binding the nickel catalyst $[Ni(P_2^{Ph}N_2^{Ph})_2](BF_4)_2$ to the acceptor end of PSI and the photocatalytic hydrogen evolution from this hybrid (Figure 1).

PSI has been the RC of choice for nature-driven photochemical hydrogen production, and in addition to the cobalt molecular catalyst,[8] PSI photochemistry has been successfully linked to catalysis from platinum clusters,[14] platinum nanoparticles,[7,15] and hydrogenase enzymes.[6,16] The key light-induced reactions in all RCs involve a series of rapid, sequential electron transfers that result in stabilized charge separation. Following photoexcitation of PSI, the primary electron donor P_{700} (a dimer of chlorophyll molecules) becomes oxidized with concurrent rapid, sequential electron transfer through a series of protein-embedded donor/acceptor molecules, terminating in electron transfer between three [4Fe-4S] clusters, F_X, F_A, and F_B.[17] PSI is poised to photochemically drive H_2 production with a long-lived $P_{700}^+F_B^-$ charge-separated state (∼60 ms) and a favorable electrochemical potential, −580 mV (vs NHE), for the F_B cluster.[5]

The nickel(II) diphosphine complex $[Ni(P_2^{Ph}N_2^{Ph})_2](BF_4)_2$[10] (Figure 2A) was found to self-assemble with native PSI (isolated from the cyanobacteria *Synechococcus leopoliensis* or *Synechococcus lividus*)[18] in aqueous solution at pH 7.3. Metal

Received: May 25, 2013
Published: August 28, 2013

dx.doi.org/10.1021/ja405277g | J. Am. Chem. Soc. 2013, 135, 13246−13249

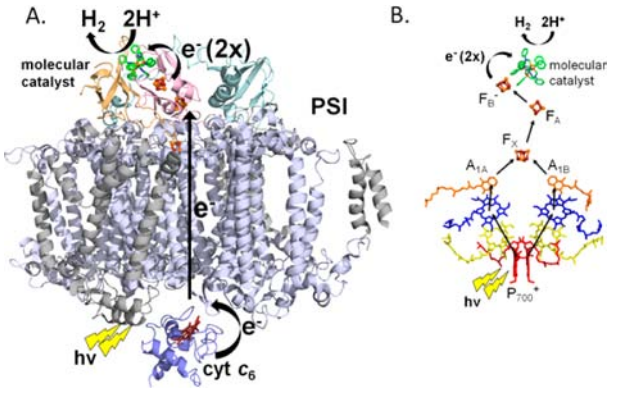

Figure 1. (A) Photocatalytic scheme of H_2 production from a PSI-Ni hybrid complex resulting from the transfer of two successive photogenerated electrons from PSI (1JB0) to a bound Ni molecular catalyst. The exact position of the Ni catalyst on the acceptor end of PSI is not known. (B) Schematic representation of the cofactors of PSI. Light-excitation initiates a series of rapid, sequential electron-transfer steps between the cofactors, resulting in the formation of the charge-separated state $P_{700}{}^{+}F_B{}^{-}$.

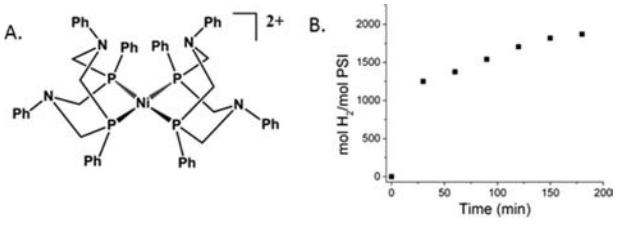

Figure 2. (A) $[Ni(P_2{}^{Ph}N_2{}^{Ph})_2]^{2+}$, the nickel diphosphine complex utilized in this study. (B) Time course profile of H_2 production of a PSI-Ni hybrid upon illumination with visible light. The assay was carried out with 80 nM PSI-Ni hybrid (1.0 Ni/PSI monomer) in 10 mM MES pH 6.3, 0.03% *n*-dodecyl *β*-D-maltopyranoside, 100 mM sodium ascorbate, and 20 *μ*M cyt c_6.

analysis of the resultant PSI-Ni complexes following removal of unbound catalyst indicates that $[Ni(P_2{}^{Ph}N_2{}^{Ph})_2](BF_4)_2$ readily binds to native PSI in ratios dependent on the initial amount of $[Ni(P_2{}^{Ph}N_2{}^{Ph})_2](BF_4)_2$ added to the protein, similar to the PSI-cobaloxime hybrid complexes.[8] Figure S1 shows metal binding results for *S. leopoliensis* and *S. lividus* protein samples that were incubated with 2−10 mol equiv of $[Ni(P_2{}^{Ph}N_2{}^{Ph})_2](BF_4)_2$ per PSI monomer in 20 mM Hepes buffer pH 7.4.

Upon illumination with visible light, H_2 formation from the self-assembled PSI-Ni catalyst hybrid is observed (Figure 2B). H_2 photocatalysis experiments were performed as previously described[8] utilizing 60−80 nM PSI monomer in 10 mM MES (pH 6.3) buffer with 0.03% *n*-dodecyl *β*-D-maltopyranoside. The final reaction mixture contained 100 mM sodium ascorbate as the sacrificial electron donor and 15−20 *μ*M cytochrome c_6 (cyt c_6) purified from *S. lividus* as the mediator to reduce $P_{700}{}^{+}$. The initial rate for H_2 production for the PSI-Ni hybrid was measured to be 0.73 mol H_2 (mol PSI)$^{-1}$ s^{-1} (turnover frequency) or 30.8 *μ*mol H_2 (mg chlorophyll)$^{-1}$ h^{-1}, observed within 30 min of illumination. As observed for a typical time course assay in Figure 2B, there is an initial burst of H_2 followed by a tapering off of H_2 evolution. H_2 production for the PSI-Ni hybrid leveled off after 3 h, with a total turnover of 1870 mol H_2/mol PSI. Samples containing 1−2 Ni per PSI monomer were found to be the most photocatalytically active. The rate of H_2 formation was investigated under a variety of conditions. The best rates were observed at pH 6.3 in 10 mM MES buffer. Lowering the pH resulted in decreased rates of H_2 formation for our hybrid system. Optimal experimental conditions for functioning of our PSI hybrid are quite distinct from the acidic conditions necessary for rapid electrocatalytic[19] and artificial photocatalytic H_2 production of $[Ni(P_2{}^{Ph}N_2{}^{Ph})_2](BF_4)_2$.[13] Hence, self-assembly of the $[Ni(P_2{}^{Ph}N_2{}^{Ph})_2](BF_4)_2$ molecular electrocatalyst with isolated PSI results in an active photochemical H_2-forming hybrid complex that functions in aqueous solution at near-neutral pH.

In an attempt to gain control over the site of Ni catalyst insertion, we investigated here a novel strategy for assembling functional PSI−molecular catalyst hybrids by using a catalyst-carrying protein. Our goal is to control molecular catalyst incorporation into a small protein and then utilize inherent protein−protein interactions to deliver catalysts in close proximity to the F_B cluster for efficient electron transfer. In Nature, PSI has two acceptor proteins, a ferredoxin (Fd) and a flavodoxin (Fld), that receive electrons from PSI and shuttle these reducing equivalents to several metabolic pathways.[20] The dynamic docking process between Fd or Fld and PSI involves electrostatic interactions of the acidic surface of the acceptor protein with a basic patch of PSI.[21] We have devised a method to insert $[Ni(P_2{}^{Ph}N_2{}^{Ph})_2](BF_4)_2$ in place of the native cofactor of Fld, a flavin mononucleotide (FMN). The FMN cofactor sits within a pocket provided by the Fld protein, but is not covalently attached to any Fld residues. FMN cofactor was removed from *S. lividus* Fld[22] by organic solvent treatment with slight modifications to reported procedures.[23−25] ApoFld was reconstituted with the $[Ni(P_2{}^{Ph}N_2{}^{Ph})_2](BF_4)_2$ catalyst during refolding of the apoprotein, forming a novel Ni-ApoFld hybrid. The catalyst must be present during the refolding procedure for creation of a hybrid complex. Metal analysis of the Ni-ApoFld hybrid demonstrates an average of 1.3 ± 0.3 Ni:Fld (10 different preparations). The binding of the Ni catalyst by the apoprotein results in a light red solution with a broad UV−vis absorption maximum at 510 nm (Figure 3A, green). Similar features are displayed by the UV−vis absorption spectrum of the $[Ni(P_2{}^{Ph}N_2{}^{Ph})_2](BF_4)_2$ catalyst in DMSO with a maximum around 475 nm (Figure 3A, brown).

To provide evidence of reversible integration of the Ni catalyst in the FMN binding pocket, we investigated the displacement of the Ni catalyst in Ni-ApoFld by addition of excess FMN. The majority of Ni-ApoFld was reconstituted with FMN, as demonstrated by UV−vis spectroscopy (Figure 3A, gray) and concurrent loss of the Ni catalyst, as evidenced by metal analysis. The spectra of native Fld (Figure 3A, black) and FMN-reconstituted Ni-ApoFld are very similar, with maxima at 465 and 372 nm.[22] Metal analysis of reconstituted Ni-ApoFld confirms loss of the $[Ni(P_2{}^{Ph}N_2{}^{Ph})_2](BF_4)_2$ catalyst, with the majority (70%) of Ni-ApoFld being reconstituted with FMN.

We have initiated electron paramagnetic resonance (EPR) studies to probe the protein−Ni catalyst hybrid structures. EPR spectroscopy is a sensitive tool for elucidating electronic structures and the surrounding environments of EPR-active species.[26] The proposed catalytic cycle of $[Ni(P_2{}^{Ph}N_2{}^{Ph})_2](BF_4)_2$ begins with reduction of Ni(II) to a Ni(I) transient state.[12] Whereas Ni(II), a $3d^8$ metal ion, is EPR silent, Ni(I) is EPR active with low spin state $S = 1/2$. The EPR spectra of PSI-Ni and Ni-ApoFld hybrids are shown in Figure 3B. The protein samples were reduced with sodium dithionite to generate the Ni(I) state. In the PSI-Ni spectra, the PSI signals of P^+, $F_A{}^-$, and $F_B{}^-$ overlap with the Ni(I) signal, as seen by

dx.doi.org/10.1021/ja405277g | J. Am. Chem. Soc. 2013, 135, 13246−13249

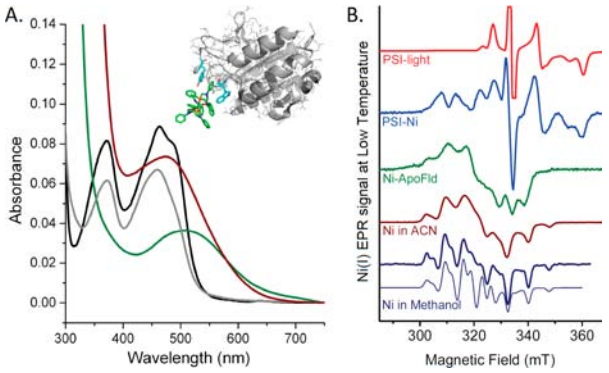

Figure 3. (A) UV−visible absorption spectra of *S. lividus* flavodoxin (black), $[Ni(P_2^{Ph}N_2^{Ph})_2](BF_4)_2$ (120 μM) in DMSO (brown), Ni-ApoFld (green), and FMN reconstituted Ni-ApoFld (gray). Protein samples were 11 μM in 20 mM Hepes pH 7.4−7.8. (Inset) Proposed model of the interaction of the Ni catalyst with the aromatic residues of flavodoxin (1CZL). (B) X-band cw EPR spectra of *S. leopoliensis* PSI (red), PSI-Ni hybrid (blue), Ni-ApoFld (green), $[Ni(P_2^{Ph}N_2^{Ph})_2](BF_4)_2$ in acetonitrile (brown), and $[Ni(P_2^{Ph}N_2^{Ph})_2](BF_4)_2$ in methanol (dark blue). Simulation (methanol) is shown as a narrow blue line using the parameters $S = 1/2$, $g = (2.111, 2.085, 2.006)$, and $A(^{31}P) = (199, 205, 214)$ MHz. Additional X-band and high-field (D-band, 130 GHz) spectra and information on the simulation are provided in the Supporting Information.

comparison with the PSI-light spectrum. Comparison of the low-field Ni(I) signals shows distinct spectral features and provides clear evidence that the Ni(I) electronic environments are quite different when the catalyst is bound to PSI or ApoFld. Spectra of PSI-Ni and Ni-ApoFld are also different from Ni(I) EPR spectra in isotropic organic solvents, like methanol or acetonitrile (Figure 3B), which is consistent with the catalyst being in different protein environments. Spectral simulations provide evidence that all of the recorded spectra demonstrate similar hyperfine interaction with four phosphorus ligands, thus confirming that the Ni diphosphine catalyst remains intact under aqueous protein environmental conditions. DFT calculations support a Ni(I) electronic state of the catalyst rather than Ni(III)-hydrides (see Supporting Information). Future detailed EPR/DFT studies of the Ni catalyst will aid in interpretation of the spectra related to catalyst structure and function in hybrid environments.

Will the Ni-ApoFld hybrid produce H_2 using the light-generated electrons of PSI? Prior to illumination, a ∼30-fold excess of Ni-ApoFld (1 Ni bound per Fld) was mixed with 80 nM PSI monomer (0 Ni bound per PSI). Visible light illumination of this mixture of Ni-ApoFld hybrid and PSI results in H_2 production rates almost 2-fold higher than observed for the PSI-Ni hybrid. The Ni-ApoFld:PSI hybrid complex displayed an initial H_2 production rate of 1.25 mol H_2 (mol PSI)$^{-1}$ s^{-1} (turnover frequency) or 52.6 μmol H_2 (mg chlorophyll)$^{-1}$ h^{-1}, observed within 20 min of illumination. H_2 production for the Ni-ApoFld:PSI hybrid complex typically leveled off after 3 h, similar to the PSI-Ni hybrid, although H_2 formation was observed at time points up to 4 h in some instances with a total turnover of 2825 mol H_2/mol PSI. Thus, Ni-ApoFld delivers the molecular catalyst to the Fld docking site of PSI, thereby facilitating successful catalyst placement for photocatalysis.

We believe that hydrophobic interactions dominate the binding of $[Ni(P_2^{Ph}N_2^{Ph})_2](BF_4)_2$ to PSI, with the catalyst tucking itself in hydrophobic pockets provided by the large PSI (∼350 kDa/monomer) protein matrix. A similar mode of binding was observed for $Co(dmgH)_2pyCl$.[8] As for interaction of $[Ni(P_2^{Ph}N_2^{Ph})_2](BF_4)_2$ with the smaller carrier protein Fld (17 kDa), experiments demonstrate that the Ni catalyst is at least partially in the FMN binding site (Figure 3A). FMN binding by Fld occurs primarily through a combination of hydrogen bonds and aromatic interactions with the apoprotein. Specifically, the indole ring of Trp 57 and the phenyl ring of Tyr 94 are critical for forming aromatic interactions with the isoalloxazine ring of FMN, and in the absence of the cofactor, these two residues collapse together.[27] This closure of the aromatic residues could explain our inability to bind the Ni catalyst to fully refolded apoprotein. If the Ni catalyst binds to Fld in a manner comparable to that of the FMN cofactor, the phenyl ligands of the catalyst could facilitate aromatic interactions with the apoprotein (Figure 3A inset). This would leave a substantial part of the bulky $[Ni(P_2^{Ph}N_2^{Ph})_2](BF_4)_2$ molecule exposed to solvent and available for interactions with hydrophobic pockets provided by PSI upon Fld docking. While electrostatic interactions help in the initial recognition and formation of protein−protein complexes for electron transfer, hydrophobic interactions play an important role in bringing the two interacting protein surfaces close enough for efficient electron transfer.[28−30] Thus, the bulky, hydrophobic Ni catalyst may actually aid in PSI-Fld complex formation. Ongoing work will investigate these interactions.

Importantly, both the PSI-Ni and Ni-ApoFld:PSI hybrid systems generate H_2 at rates 2 orders of magnitude greater than rates (0.0056 mol H_2 (mol catalyst)$^{-1}$ s^{-1}) reported for photosensitizer/$[Ni(P_2^{Ph}N_2^{Ph})_2](BF_4)_2$ systems.[13] Our hybrids reaffirm the usefulness of Nature's optimized RC photon capture and charge-separation capabilities to drive photocatalysis at molecular catalyst sites. To function, these systems must successfully couple single-electron photoexcited states with the multiple proton-coupled electron-transfer reactions at the metal-centered catalyst sites; we have achieved this coupling via self-assembly of the catalyst with PSI or delivery of catalyst to PSI via ApoFld. The PSI-Ni hybrid resulted in a total turnover number of 1870 mol H_2/mol PSI in 3 h. Utilizing the Ni-ApoFld hybrid to transfer the catalyst to PSI demonstrated a higher turnover number of 2825 mol H_2/mol PSI in 4 h, comparable to the total turnover number of 2700 reported for the $[Ni(P_2^{Ph}N_2^{Ph})_2](BF_4)_2$ catalyst with the synthetic photosensitizers Eosin Y and $[Ru(bpy)_3]^{2+}$ obtained in 150 h performed in 1:1 water:acetonitrile mixtures at pH 2.25.[13] Thus, the duration of photocatalysis is much longer for the photosensitizer system than our PSI hybrids. Metal analysis indicates that >90% of the $[Ni(P_2^{Ph}N_2^{Ph})_2](BF_4)_2$ catalyst has dissociated from the protein following photocatalysis of the PSI-Ni hybrid (no Fld present), similar to previous findings with the PSI-cobaloxime hybrid.[8] For PSI-Ni hybrid, it is unclear if the catalyst is simply falling off PSI or if the catalyst is degrading and then dissociating from the protein. We are currently investigating a role for the dynamic interaction between PSI and ApoFld in protecting the catalyst from solvent exposure and the molecular transfer of catalyst from Ni-ApoFld to dissociated catalyst sites on PSI.

The pendant amines of $[Ni(P_2^{Ph}N_2^{Ph})_2](BF_4)_2$ provide rate-accelerating proton relays for metal hydride formation, facilitating formation of hydrogen via a low-energy pathway.[10,12,31] Strong acids such as protonated dimethyl formamide ($DMFH^+$) are necessary for rapid electrocatalysis by $[Ni(P_2^{Ph}N_2^{Ph})_2](BF_4)_2$, which produces H_2 at rates >350 s^{-1}

dx.doi.org/10.1021/ja405277g | J. Am. Chem. Soc. 2013, 135, 13246−13249

in acetonitrile.[19] Our work demonstrates the finding that protein binding sites in PSI allow these catalysts to be used for hydrogen production at neutral pH. The −0.20 V Ni(II/I) $[Ni(P_2^{Ph}N_2^{Ph})_2](BF_4)_2$ reduction potential (vs NHE) in acetonitrile[10] is in a favorable range for electron transfer from the F_B cluster of PSI but results in an underpotential for H_2 catalysis. However, both Ni-PSI and Ni-ApoFld hybrids produce H_2; thus, the protein environments must alter the Ni(II/I) potential of $[Ni(P_2^{Ph}N_2^{Ph})_2](BF_4)_2$. Future work will address the protein effects on molecular catalyst reduction potentials in biohybrid systems.

In summary, we have prepared the first solar fuel hybrid that utilizes Nature's optimized photochemistry to drive H_2 production from a nickel molecular catalyst, $[Ni(P_2^{Ph}N_2^{Ph})_2](BF_4)_2$, in completely aqueous conditions at near-neutral pH. Additionally, we demonstrate a novel strategy for creation of solar fuel hybrids that involves delivery of a molecular catalyst via ApoFld to the reducing end of PSI for light-driven catalysis. The ability of ApoFld to incorporate non-native cofactors into the FMN binding site can be exploited in future hybrid designs by utilizing ligands that promote interactions between synthetic molecular catalysts and apoprotein. This approach provides the potential for self-repair of the biohybrid system with a mechanism for introducing fresh catalyst to the acceptor end of PSI. This work presents new exciting opportunities to link synthetic designs with Nature's inherent RC photochemistry for photocatalytic H_2 production utilizing earth-abundant materials.

■ ASSOCIATED CONTENT

Supporting Information

Experimental methods, metal binding and H_2 production data, H_2 control experiments, X-band and D-band EPR spectra, and computer simulation parameters. This material is available free of charge via the Internet at http://pubs.acs.org.

■ AUTHOR INFORMATION

Corresponding Author

tiede@anl.gov; utschig@anl.gov

Present Address

[†]P.D.: CAS Key Laboratory of Materials for Energy Conversion & Department of Materials Science & Engineering, University of Science and Technology of China (USTC), Hefei, Anhui 230026, P. R. China

Notes

The authors declare no competing financial interest.

■ ACKNOWLEDGMENTS

We thank A. Wagner for growth of the cyanobacteria and K. L. Mulfort and M. C. Thurnauer for critical reading of the manuscript. This work is supported by the Division of Chemical Sciences, Geosciences, and Biosciences, Office of Basic Energy Sciences of the U.S. Department of Energy under Contract DE-AC02-06CH11357.

■ REFERENCES

(1) Lewis, N. S. *Science* **2007**, *315*, 798−801.
(2) Lewis, N. S.; Nocera, D. G. *Proc. Natl. Acad. Sci. U.S.A.* **2006**, *103*, 15729−15735.
(3) Nocera, D. G. *Inorg. Chem.* **2009**, *48*, 10001−10017.
(4) Blankenship, R. E. *Molecular Mechanisms of Photosynthesis*; Blackwell Science Ltd.: Malden, MA, 2002.
(5) Lubner, C. E.; Grimme, R.; Bryant, D. A.; Golbeck, J. H. *Biochemistry* **2010**, *49*, 404−414.
(6) Lubner, C. E.; Applegate, A. M.; Knorzer, P.; Ganago, A.; Bryant, D. A.; Happe, T.; Golbeck, J. H. *Proc. Natl. Acad. Sci. U.S.A.* **2011**, *108*, 20988−20991.
(7) Utschig, L. M.; Dimitrijevic, N. M.; Poluektov, O. G.; Chemerisov, S. D.; Mulfort, K. L.; Tiede, D. M. *J. Phys. Chem. Lett.* **2011**, *2*, 236−241.
(8) Utschig, L. M.; Silver, S. C.; Mulfort, K. L.; Tiede, D. M. *J. Am. Chem. Soc.* **2011**, *133*, 16334−16337.
(9) Trogler, W. C.; Stewart, R. C.; Epps, L. A.; Marzilli, L. G. *Inorg. Chem.* **1974**, *13*, 1564−1570.
(10) Wilson, A. D.; Newell, R. H.; McNevin, M. J.; Muckerman, J. T.; Rakowski DuBois, M.; DuBois, D. L. *J. Am. Chem. Soc.* **2006**, *128*, 358−366.
(11) Rakowski DuBois, M.; DuBois, D. L. *Acc. Chem. Res.* **2009**, *42*, 1974−1982.
(12) Helm, M. L.; Stewart, M. P.; Bullock, R. M.; Rakowski DuBois, M.; DuBois, D. L. *Science* **2011**, *333*, 863−866.
(13) McLaughlin, M. P.; McCormick, T. M.; Eisenberg, R.; Holland, P. L. *Chem. Commun.* **2011**, *47*, 7989−7991.
(14) Iwuchukwau, I. J.; Vaughn, M.; Myers, N.; O'Neill, H. M.; Frymier, P.; Bruce, B. D. *Nat. Nanotechnol.* **2010**, *5*, 73−79.
(15) Grimme, R. A.; Lubner, C. E.; Bryant, D. A.; Golbeck, J. H. *J. Am. Chem. Soc.* **2008**, *130*, 6308−6309.
(16) Ihara, M.; Nishihara, H.; Yoon, K. S.; Lenz, O.; Friedrich, B.; Nakamoto, H.; Kojima, K.; Honma, D.; Kamachi, T.; Okura, I. *Photochem. Photobiol.* **2006**, *82*, 676−682.
(17) Golbeck, J. H. *Photosystem I: The Light-Driven Plastocyanin:Ferredoxin Oxidoreductase*; Springer: Dordrecht, The Netherlands, 2006.
(18) Utschig, L. M.; Chen, L. X.; Poluektov, O. G. *Biochemistry* **2008**, *47*, 3671−3676.
(19) Wilson, A. D.; Shoemaker, R. K.; Miedaner, A.; Muckerman, J. T.; DuBois, D. L.; Rakowski DuBois, M. *Proc. Natl. Acad. Sci. U.S.A.* **2007**, *104*, 6951−6956.
(20) Setif, P. *Biochim. Biophys. Acta* **2001**, *1507*, 161−179.
(21) Medina, M. *FEBS J.* **2009**, *276*, 3942−3958.
(22) Crespi, H. L.; Smith, U.; Gajda, L.; Tisue, T.; Ammeraal, R. M. *Biochem. Biophys. Acta* **1972**, *256*, 611−618.
(23) Edmondson, D. E.; Tollin, G. *Biochemistry* **1971**, *10*, 124−132.
(24) Genzor, C. G.; Beldarrain, A.; Gomez-Moreno, C.; Lopez-Lacomba, J. L.; Cortijo, M.; Sancho, J. *Protein Sci.* **1996**, *5*, 1376−1388.
(25) Hu, Y. F.; Li, Y.; Zhang, X. X.; Guo, X. R.; Xia, B.; Jin, C. W. *J. Biol. Chem.* **2006**, *281*, 35454−35466.
(26) Niklas, J.; Mardis, K. L.; Rakhimov, R. R.; Mulfort, K. L.; Tiede, D. M.; Poluektov, O. G. *J. Phys. Chem. B* **2012**, *116*, 2943−2957.
(27) Genzor, C. G.; Perales-Alcon, A.; Sancho, J.; Romero, A. *Nat. Struct. Biol.* **1996**, *4*, 329−332.
(28) Morales, R.; Charon, M. H.; Kachalova, G.; Serre, L.; Medina, M.; Gomez-Moreno, C.; Frey, M. *EMBO Rep.* **2000**, *1*, 271−276.
(29) Kurisu, G.; Kusunoki, M.; Katoh, E.; Yamazaki, T.; Teshima, K.; Onda, Y.; Kimata-Ariga, Y.; Hase, T. *Nat. Struct. Biol.* **2001**, *8*, 117−121.
(30) Goni, G.; Serrano, A.; Frago, S.; Hervas, M.; Peregrina, J. R.; De la Rosa, M. A.; Gomez-Moreno, C.; Navarro, J. A.; Medina, M. *Biochemistry* **2008**, *47*, 1207−1217.
(31) Kilgore, U. J.; Roberts, J. A. S.; Pool, D. H.; Appel, A. M.; Stewart, M. P.; DuBois, M. R.; Dougherty, W. G.; Kassel, W. S.; Bullock, R. M.; DuBois, D. L. *J. Am. Chem. Soc.* **2011**, *133*, 5861−5872.